

RESEARCH ARTICLE

Secondary chain motion and mechanical properties of γ -irradiated-regenerated cellulose films

Aisha Tanvir, Mariam A. Al-Maadeed and Mohammad K. Hassan

Center for Advanced Materials, Qatar University, Doha, Qatar

Regenerated cellulose films prepared using NaOH/urea solvent system were exposed to different doses of γ -radiation, ranging from 5 to 50 kGy to modify their properties. Change in relative crystallinity as a function of absorbed dose was studied using XRD. The tensile and dynamic mechanical properties were tested and it was found that exposure to 10 kGy imparted maximum improvement in these properties, that is 10% improvement in tensile strength, 43% increase in Young's modulus, and 22% increase in storage modulus. Broadband dielectric spectroscopy technique was used to investigate effect of absorbed dose on the secondary chain motions of the regenerated cellulose and the results were in line with findings of the tensile and dynamic mechanical tests.


Received: December 2, 2015

Revised: December 24, 2015

Accepted: January 13, 2016

Keywords:

γ -radiation / Dielectric spectroscopy / Mechanical properties / Regenerated cellulose / Secondary chain motion

 Additional supporting information may be found in the online version of this article at the publisher's web-site.

1 Introduction

Cellulose is a truly sustainable natural polymer increasingly being used in various industries including the pharmaceutical, packaging, and food industry as a superior environmentally friendly alternative to conventional materials [1–3]. Its exceptional mechanical properties also make it a suitable reinforcement material for polymer composites [4, 5].

Cellulose serves as the main constituent in plant cell walls; it is a linear polysaccharide consisting of numerous glucose units held together by β -(1,4)-D-glycosidic linkages [6]. Among the most noteworthy properties of cellulose are its biodegradability and high mechanical and thermal stability [7]. However, despite the aforementioned properties, utilization of cellulose is far below its potential. This is mainly due to its insolubility in common solvents caused by strong intra- and intermolecular hydrogen bonding [8]. The key to dissolving cellulose is to disrupt the extensive hydrogen bonding which holds the chains together. Over the years, a number of solvent systems have been developed

and reported to successfully dissolve cellulose. These include N-methylmorpholine N-oxide (NMMO) monohydrate [9], N, N-dimethylacetamide (DMAc)/LiCl [10], and ionic liquids [11]. While these solvents are able to dissolve cellulose, they are far from being employed at an industrial scale due to their high cost, the inability to recover solvent, and instability.

A more feasible solvent reported is the mixture of NaOH/urea aqueous solution [12]; it exhibits rapid dissolution of cellulose at low temperatures and is exceptionally economical as well as environmentally friendly. NaOH/urea aqueous solution acts as a non-derivatizing solvent, which breaks the intra- and intermolecular hydrogen bonding in cellulose and forms a cellulose inclusion complex resulting in a homogeneous cellulose solution. Upon adding a coagulant (non-solvent) to the cellulose solution, the inclusion complex is destroyed resulting in self-association of the cellulose chains through formation of new –OH groups, which results in a variety of “regenerated” cellulosic products [13].

Modification of natural polymers using γ -radiation has been on the rise as radiation being a physical process is more economically viable and less toxic than chemical processes. Exposure of polymeric materials to ionic radiation (γ -rays, electron beams, ion beams, X-rays) can significantly alter the

Correspondence: Prof. Mariam A. Al-Maadeed, Center for Advanced Materials, Qatar University, P.O. Box 2713, Doha, Qatar
E-mail: m.alali@qu.edu.qa
Fax: +974 4403-3989

Abbreviations: DMA, dynamic mechanical analyzer; FTIR, Fourier transform infrared spectroscopy; XRD, X-ray diffraction

Colour Online: See the article online to view figures in colour.

physical and chemical characteristics of the polymer [14]. γ -Irradiation can be used for sterilization of the materials for applications related to food packaging or medical devices. Ionizing radiation upon interaction with polymers produces free radicals, ions, and highly reactive excited states; all of which can participate in several possible reactions including chain scission (degradation), cross-linking, chain aggregation, sterilization, grafting, and oxidation reactions [14–16]. Radiation-induced modification of natural polymers includes generation of starch nanoparticles by γ -irradiation of cassava and waxy maize [17]. Grafting of a monomer, 2-butane diol-diacrylate on chitosan-starch-based films [18]. Degradation of chitosan-based aqueous solutions and films [19]. Hydrogel formation of collagen upon exposure to γ -radiation [20].

Previous work related to the effect of γ -radiation on cellulose includes investigation of the effect of γ -irradiation and alkali treatment on cotton cellulose [21]. The authors reported structural changes, increase in the carbonyl content, and transformation from cellulose I to cellulose II. In another study, the effect of various doses of γ -irradiation on transport parameters, surface chemistry, and electrical properties of regenerated cellulose membranes was studied; modification in the OH moieties, a decrease in electrical resistance, and reduction in the free volume of the material was reported [22].

However, an investigation of the effect of γ -irradiation on the mechanical and electrical properties of regenerated cellulose has not been reported yet. Therefore, the aim of this contribution is to study alterations caused by γ -irradiation in the aforementioned properties. Regenerated cellulose films were prepared using the NaOH/urea solvent system and subsequently exposed to γ -radiation ranging from 5 to 50 kGy. The irradiated films were analyzed using Fourier transform infrared spectroscopy (FTIR), dynamic mechanical analyzer (DMA), X-ray diffraction (XRD), and broadband dielectric spectroscopy (BDS) to study the effect of γ -radiation on the mechanical and electrical properties of the films. Mauritz and Hassan have used broadband dielectric spectroscopy (BDS) to interrogate dynamics of chain motions and chemical degradation in polylactides and Nafion[®] membranes [23–25]. BDS is a powerful tool of interrogation as information regarding motional processes can be collected over broad time and distance scales [26]. In addition to polymer relaxations, details on differences in dielectric permittivity and/or charge conductivity across phase boundaries, which cause fluctuating interfacial polarization, can be detected in great details [27].

2 Materials and methods

2.1 Materials

Microcrystalline cellulose was purchased from Sigma–Aldrich. All the reagents (NaOH, urea, H₂SO₄, and Na₂SO₄)

were of analytical grade and bought from BDH Chemicals, UK. They were used as received without further purification. Deionized water was used throughout the experiment.

2.2 Preparation of regenerated cellulose films

Cellulose solution was prepared according to a previously reported method [12]. An aqueous solution of 6 wt% NaOH/4 wt% urea was cooled to -12°C . A known amount of cellulose powder was subsequently added to this solution accompanied by vigorous stirring for 15–20 min at ambient temperature until a homogenous cloudy solution with concentration of 4 wt% was obtained. The solution was again cooled to -5°C for about 5 h, and then thawed with intermittent mixing at $0\text{--}4^{\circ}\text{C}$ to obtain a transparent solution. This cellulose solution was then centrifuged at 6000 rpm for 20 min to carry out degasification and to remove any undissolved residuals.

The resulting solution was cast onto a glass plate to have a thickness of 0.20–0.30 mm and then immediately coagulated in 5 wt% Na₂SO₄ aqueous solution for 5 min to obtain transparent films. The prepared films were extensively washed with water until they reached pH 7, then dried at room temperature for 48 h. The films were further dried in a desiccator containing calcium chloride at room temperature for 3 days.

2.3 Radiation of regenerated cellulose films

The regenerated cellulose films were irradiated by γ -ray using a ⁶⁰Co γ -cell manufactured by Atomic Energy of Canada Co., Ltd. The films were exposed to γ -irradiation of dosages 5, 10, 20, and 50 kGy at a dose rate of 1.8 kGy/h; irradiation was carried out at room temperature under air atmosphere.

2.4 Irradiated films characterization

2.4.1 Fourier transform infrared spectroscopy (FT-IR)

The FT-IR spectra of the films were measured using a Perkin Elmer Spectrum 100. The FT-IR spectra were recorded using 32 scans in the range of $500\text{--}4000\text{ cm}^{-1}$ at a resolution of 4 cm^{-1} .

2.4.2 X-ray diffraction measurements (XRD)

X-ray diffraction studies were performed using an XRD diffractometer (Mini Flex 2, Rigaku). Nickel filtered CuK α radiation ($\lambda = 0.1564\text{ nm}$) operated at 30 V and 15 mA served as the source. XRD patterns were recorded in the 2θ range of $5\text{--}35^{\circ}$ at a scanning speed of $1.8^{\circ}/\text{min}$. The relative crystallinity χ_C (%) of the regenerated cellulose films was estimated using the peak deconvolution method, as per the

following equation:

$$\text{Crystallinity}\% = \frac{A_c}{A_c + A_a} \quad (1)$$

where A_c is the area of the crystalline diffraction peak, whereas A_a is the area of the amorphous diffraction peak.

2.4.3 Tensile testing

The tensile properties of the films were measured using the RSA-G2 (TA Instruments, USA) according to ASTM D 882-10 at 25°C and at crosshead speed of 5.0 mm/min. Rectangular specimens were cut with dimension of 30 mm \times 5 mm \times 0.03 mm. Five specimens of each sample were tested; the tensile strength, elongation at break and Young's modulus were calculated as an average of five measurements to ensure data accuracy.

2.4.4 Dynamic mechanical analysis (DMA)

Dynamic mechanical analysis was conducted using RSA-G2 (TA Instruments, USA) in tensile mode at 25°C and air atmosphere. Rectangular samples of dimensions 25 mm \times 5 mm \times 0.03 mm were prepared and measured in linear viscoelastic range. The mechanical response was investigated in the frequency range of 0.1–100 Hz at strain deformation of 0.01%.

2.4.5 Broadband dielectric spectroscopy

Dielectric measurements on the C₆₀-thiol-ene network films were performed using a Novocontrol GmbH Concept 40 broadband dielectric spectrometer, and data were collected over the frequency range of 0.1 Hz to 3 MHz and temperature range of –90 to 220°C. Samples were kept in a desiccator at room temperature for more than 1 week before the dielectric experiments to minimize the obscuring influence of water on the dielectric response. Sample discs of 2 cm diameter were sandwiched between two gold-coated copper electrodes of 2 cm diameter and transferred to the instrument for data collection. The sample loading process took \cong 5 min. The following Havriliak–Negami (H–N) equation [28–30] was fitted to experimental data to extract dielectric parameters related to the sub- T_g motions:

$$\begin{aligned} \varepsilon^*(\omega) &= \varepsilon' - i\varepsilon'' \\ &= -i \left(\frac{\sigma_{dc}}{\varepsilon_0 \omega} \right)^N + \sum_{k=1}^3 \left[\frac{\Delta\varepsilon_k}{(1 + (i\omega\tau_{HN})^{\alpha_k})^{\beta_k}} + \varepsilon_{\infty k} \right] \end{aligned} \quad (2)$$

where ε' and ε'' are the real and imaginary dielectric permittivities, respectively, and $i^2 = -1$. Equation (2) has three relaxation terms in the sum and a term on the left accounts for dc conductivity. ε_0 = vacuum permittivity and $\omega = 2\pi f$. For each relaxation term k , the dielectric strength

$\Delta\varepsilon_k = (\varepsilon_R - \varepsilon_{\infty})_k$ is the difference between ε' at very low and very high frequencies, respectively. σ_{dc} is dc conductivity and the exponent N characterizes conduction in terms of the nature of charge hopping pathways and charge mobility constraints. α and β characterize the breadth and degree of asymmetry, respectively, of ε'' versus ω peaks. The Havriliak–Negami relaxation time τ_{HN} is related to the actual relaxation time τ_{max} at loss peak maximum at f_{max} by the following equation [31]:

$$\tau_{max} = \tau_{HN} \left[\frac{\sin\left(\frac{\pi\alpha\beta}{2(\beta+1)}\right)}{\sin\left(\frac{\pi\alpha}{2(\beta+1)}\right)} \right]^{\frac{1}{\alpha}} \quad (3)$$

The dc term in Eq. (3) accounts for inherent or unintended (impurity) charge migration that is often subtracted to uncover loss peaks or at least make them more distinct.

3 Results and discussion

3.1 FT-IR analysis

FT-IR was used to investigate any possible changes in the chemical structure caused by γ -irradiation. The IR spectra (Supporting Information Fig. S1) of the irradiated films were similar to that of the non-irradiated film indicating that no other structural changes occurred besides weakening of hydrogen bonds due to irradiation.

All the samples exhibited a broad absorption band at 3200–3400 cm⁻¹ which is assigned to the stretching vibrations of the O–H group. The band narrowed with increasing irradiation dosage, suggesting weakening of the intermolecular hydrogen bonding. This observation is consistent with previous reports in the literature [22].

In addition, all films exhibited absorption bands characteristic to regenerated cellulose, including CH₂ vibration at 2700–2900 cm⁻¹, C–O carbonyl stretching at 1654 cm⁻¹, O–H bending vibrations at 1372 cm⁻¹, C–O bond stretching vibration at 1200 cm⁻¹. A sharp peak was observed at 894 cm⁻¹ which is characteristic of β -glycosidic linkages between glucose molecules in cellulose and is restricted to regenerated cellulose [11].

3.2 XRD analysis

XRD analysis was performed to study the change in relative crystallinity of the films upon exposure to γ -irradiation. The XRD patterns of the regenerated films exposed to different doses of radiation are shown in Fig. 1. All the films showed typical cellulose II structure with peaks at \sim 12, 20, 22°, which are assigned to the (110), (110), and (200) planes [32].

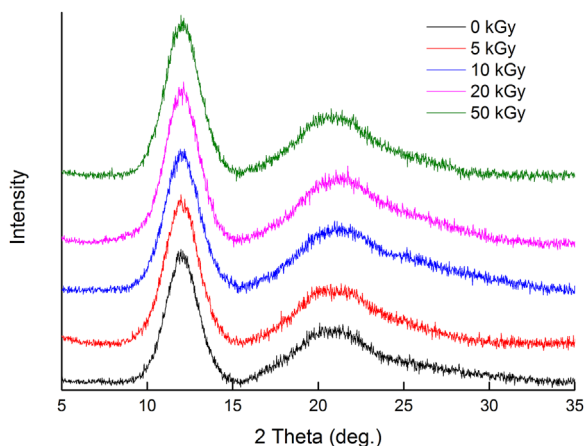


Figure 1. XRD diffraction patterns of the regenerated cellulose films exposed to different radiation doses.

The effect of γ -irradiation on the relative crystallinity (χ_c , %) of the regenerated cellulose films was calculated using the peak deconvolution method. The results illustrated that low dosage of radiation of 5 and 10 kGy increased the relative crystallinity up to 12%; however, at higher dosage of 20 and 50 kGy, the relative crystallinity percentage decreased up to 20%. The slight increase in relative crystallinity at low doses is possibly due to improved arrangement of the cellulose chains due to γ -radiation induced cross-linking. Whereas, at doses above 10 kGy relative crystallinity decreases up to 20%, this may be attributed to chain scission, which occurs preferentially in the amorphous regions and reduces crystallinity. A similar trend of cross-linking at low doses, followed by chain scission at high doses, was observed in the tensile and dynamic mechanical analysis results as reported below; this was also previously reported by Takacs *et al.* [21].

3.3 Tensile testing

Upon exposure of cellulosic materials to radiation, the production of radicals on the cellulose chain (due to hydrogen and hydroxyl abstraction) occurs. In addition, cleavage of glycosidic bonds occurs by random depolymerization leading to a decrease in the molecular weight. A correlation exists between the concentration of free radicals formed in irradiated cellulose and irradiation dosage. At lower doses (≤ 10 kGy) cellulose chains undergo crosslinking whereas at higher doses, degradation by chain scission predominates [33–35].

Regenerated cellulose films were exposed to γ -radiation at doses varying from 0 to 50 kGy. Their tensile properties were then investigated as seen in Fig. 2 and Table 1.

The results depicted an increase in the tensile strength at doses up to 10 kGy, whereas doses above 10 kGy induced a decrease in tensile strength. At 10 kGy, the films reached a tensile strength value of 68.30 MPa, which is 10% higher

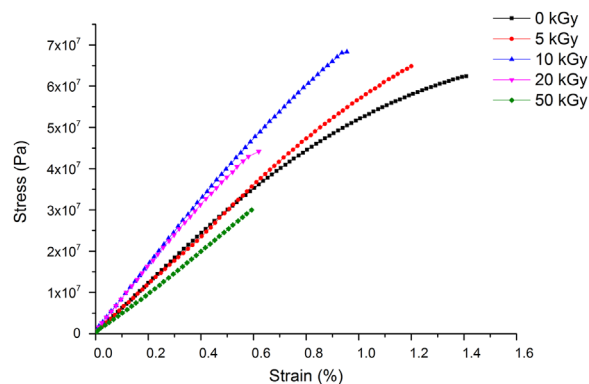


Figure 2. Stress–strain curve of the non-irradiated and irradiated regenerated cellulose films.

than the non-irradiated control sample. However, at doses higher than 10 kGy, the tensile strength values decreased.

At low-absorbed dose, an improvement in mechanical properties is seen which is likely to be caused by cross-linking, which results in a stronger but brittle material. However, at higher, chain scission appears to be dominant over cross-linking which results in reduction of the molecular weight and henceforth loss in mechanical properties. In addition, γ -irradiation reduced elasticity of the films as observed by reduction in the elongation at break. This reduction further indicates that γ -irradiation induces cross-linking between the polymer chains, which reduced polymer chain mobility as well as elasticity.

In γ -irradiation, the phenomena of cross-linking and chain scission occur simultaneously but at different rates. The phenomenon that is dominant at a given dose determines the manner in which materials mechanical properties are altered.

Similar observations of improvement in mechanical properties at low doses of γ -irradiation, followed by loss in properties at higher doses have been reported previously [36, 37].

3.4 Dynamic mechanical analysis

Influence of γ -irradiation dosage on the viscoelastic properties of the regenerated cellulose films were studied

Table 1. Mechanical properties of the non-irradiated and irradiated regenerated cellulose films

Absorbed dose (kGy)	Tensile strength (MPa)	Elongation at break (%)	Young's modulus (MPa)
0	62.37 ± 5.36	1.41 ± 0.19	56.44 ± 4.38
5	67.51 ± 7.01	1.29 ± 0.23	60.73 ± 5.65
10	68.30 ± 6.54	0.95 ± 0.23	80.44 ± 5.46
20	44.16 ± 8.31	0.62 ± 0.09	77.95 ± 5.01
50	30.00 ± 5.90	0.59 ± 0.06	50.06 ± 7.99

by DMA. The frequency dependence of the dynamic storage (G') and loss modulus (G'') at 25°C is shown in Fig. 3(a).

Absorbed dose of up to 10 kGy improved the elasticity and increased the storage modulus within the entire frequency range. This increase may be due to decreased chain mobility caused by crosslinking between the polymer chains. Absorbed dose of more than 10 kGy depicted reduction in the storage modulus possibly due to the scission of the polymer chains, which is more pronounced after 10 kGy dose. The dependence of the loss modulus on the absorbed dose is shown in Fig. 3(b). The variation of this parameter is similar to the storage modulus as the minimum is achieved at 10 kGy. The improvement of the loss modulus from the application point of view is a crucial parameter. It indicates that heat dissipation upon mechanical deformation is rather low for films irradiated at 10 kGy, whereas films irradiated at 50 kGy exhibit high loss modulus implying that huge amount of mechanical energy is converted to heat resulting in loss of mechanical properties.

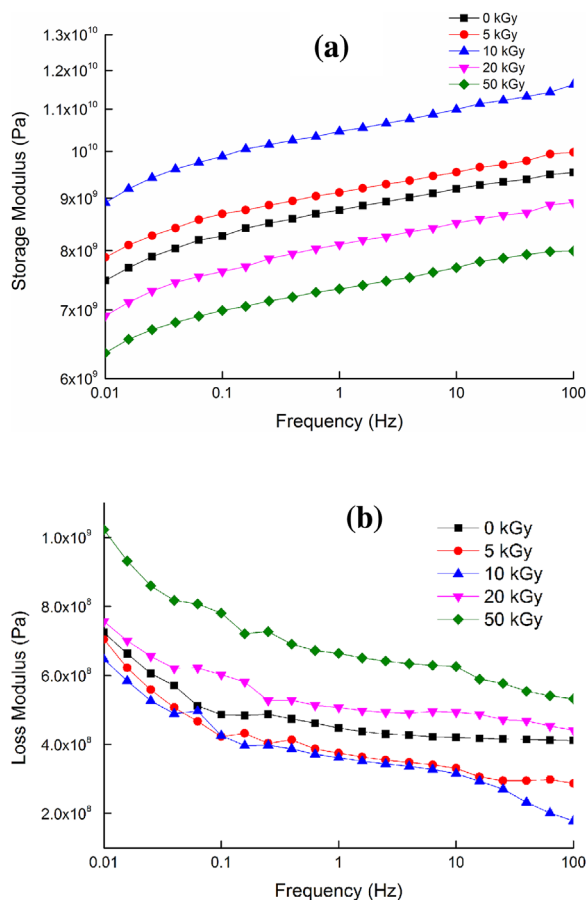


Figure 3. Frequency dependence of the dynamic storage (a) and loss (b) modulus of the films.

3.5 Dielectric spectroscopy measurements

The dielectric spectra of amorphous polymers usually exhibit relaxations at different temperatures (T), where each is designated by a peak in the ϵ'' versus f curves and a rapid decline in storage permittivity ϵ' versus f curves at a fixed T . The dynamic dielectric response was reported to be sensitive to alterations in the fine structure of cellulose [38]. In a control regenerated cellulose film, two relaxations are evident as shown by the 3D $\epsilon''-f-T$ surface (Supporting Information Fig. S2). Of interest in this study is the sub- T_g relaxations usually kick in at very low temperatures. These relaxations are associated with the movement of the lateral CH_2OH groups, γ -relaxation, and localized movements of glucose units facilitated by the presence of flexible glycosidic linkages, β -relaxation [39]. Analysis of the effect of γ -irradiation on the T_g relaxation, related to long-range chain segmental mobility and which kicks in around room temperature, will be a subject of a future publication. The linear monotonic uplift of ϵ'' values at low f accounts for the dc conduction due to the presence of ionic impurities, e.g., NaOH and Na_2SO_4 used during the film preparation step. At low f , charge hopping events will have enough time to be sampled during the experimental time scale of a half period of oscillation $(2f)^{-1}$ and before the applied electric field reverses. Above the T_g , ionic impurity motion will be greater due to increased chain segmental mobility at the onset of the glass transition.

Figure 4 shows the ϵ'' versus f spectra of the control and 50 kGy-irradiated samples within the sub- T_g temperature range. The control sample shows the presence of a γ -relaxation peak with its maxima shift to higher frequencies as the temperature increases in a typical way. The solid lines represent the H-N model fits to the spectra. Whereas for the 50 kGy-sample, both the γ - and β -relaxations are evident. Comparison of the spectra at -50°C for all samples reveals the presence of the β -relaxation as a weak shoulder within the low frequency side for the 10 and 20 kGy samples (Fig. 5). While this shoulder develops to a well-resolved peak for the 50 kGy sample. The position of the γ - and β -relaxation peak maxima does not shift to low or high frequency values indicating that these transitions exhibit the same relaxation times regardless of the irradiation.

The relaxation times (τ_{max}) extracted from fitting the spectra to the H-N model reveal an Arrhenius behavior as illustrated in Fig. 6. The activation energies (E_a) values for this motion were extracted using the Arrhenius equation and are listed in Table 2:

$$\tau_{\text{max}}(T) = \tau_0 \exp\left(\frac{E_a}{RT}\right) \quad (4)$$

where R is the universal gas constant and τ_0 is a pre-exponential factor. The activation energies shown in Table 2 for the γ -relaxation motion decreased with irradiation. This

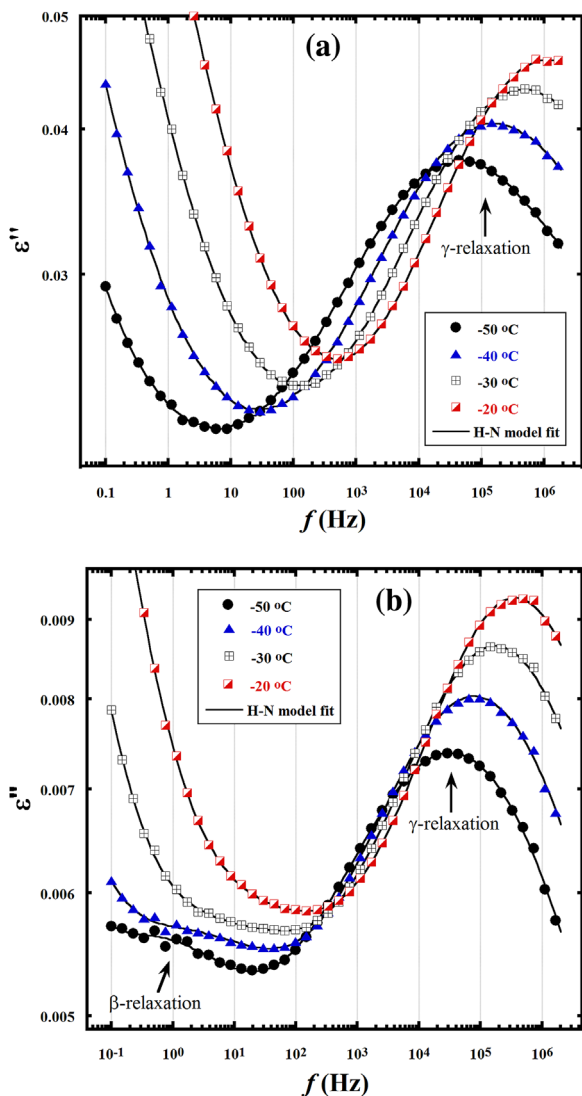


Figure 4. ϵ'' versus f plots for the non-irradiated control (a) and 50 kGy-irradiated (b) samples, within the sub- T_g temperature range. Lines represent the H–N equation fits to the spectra.

lowering would reflect the ease of the rotation motion of the CH_2OH groups with irradiation. It is also in agreement with the above-noted result of decreased relative crystallinity of the samples at higher dosage of radiation. Therefore, the γ -relaxation motion in case of the 50 kGy sample required the least amount of energy, 39.6 kJ mol^{-1} , to be activated due to its enhanced amorphous character [40].

The β -relaxation showed a much higher activation energy value of 76.3 kJ mol^{-1} . This relaxation is associated with local movements of segments of the main polymer chain and involves glucose rings rotation around a number of glycosidic linkages [39]. For an amorphous cellulose sample having a degree of polymerization of 20, the energy barrier for this relaxation was found to be in the order of 20 kJ mol^{-1} [39]. A plausible explanation of such high

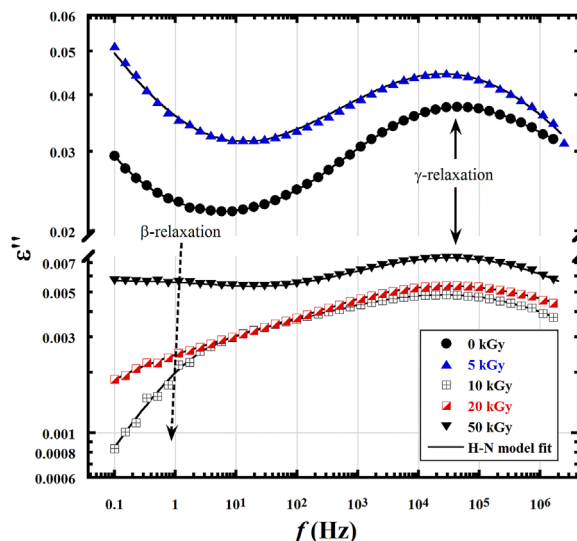


Figure 5. ϵ'' versus f spectra at -50°C for the irradiated and non-irradiated control regenerated cellulose samples, showing the β - and γ -relaxations. Lines represent the H–N equation fits to the spectra.

activation energy for the local segmental motion in the 50 kGy sample is that degradation caused the cracking of chain segments having a degree of polymerization of about 70. This conclusion requires further evidence as other parameters such as crosslinking would cause the activation energy for the local movements of segments to rise.

A table summarizing the dielectric parameters of the γ -relaxation peak, which are extracted from fitting the spectra of the samples to the H–N equation can be found in Supporting Information Table S1. The dielectric strength

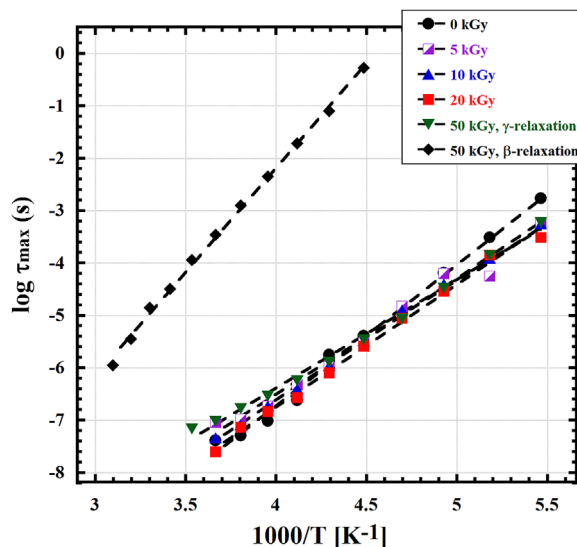


Figure 6. Arrhenius plots of the γ -relaxation (all samples) and β -relaxation (50 kGy sample only), for a series of regenerated cellulose films exposed to different radiation doses as well as a control non-irradiated sample.

Table 2. Calculated activation energies for the γ - and β -relaxations of the regenerated cellulose films as a function of the absorbed dose

Absorbed dose (kGy)	E_a (kJ/mol)	Fit R^2
0	51.4	0.99633
5	41.6	0.99056
10	44.3	0.99931
20	44.6	0.99775
50 (γ -relaxation)	39.6	0.99689
50 (β -relaxation)	76.3	0.99894

($\Delta\epsilon$) values for this process in the 50 kGy irradiated sample are almost one decade lower than those for the untreated control at all temperatures. This may seem counter intuitive as it is expected that CH_2OH groups would exhibit more dipolar activity because of facilitated motions due to above-mentioned reduced relative crystallinity and lower activation energy for the γ -relaxation of the 50 kGy irradiated sample. However, other factors might contribute to the dielectric strength reduction of these motions such as crosslinking, residual moisture, and morphological alterations [40]. One or more of these irradiation effect were marked in the mechanical tensile, dynamic mechanical analysis, and SEM results for the samples reported in this work.

4 Concluding remarks

An economic and efficient method to modify properties of regenerated cellulose films was achieved using γ -irradiation of specific dosage. An optimum dosage of 10 kGy was found to be effective in improving the tensile, dynamic mechanical properties of the regenerated cellulose films. Samples exposed to 10 kGy depicted uniform and smooth surface without any noticeable cracks or voids. Additionally, 10% improvement in tensile strength, 43% increase in Young's modulus, and 22% increase in storage modulus was observed at a dose of 10 kGy.

Dielectric analysis of the sub- T_g region revealed a drop in the activation energy for the γ -relaxation associated with the CH_2OH groups' lateral motions. This drop is in agreement with the decrease in relative crystallinity at high-absorbed doses, which would facilitate the rotation of the CH_2OH groups, and the energy required for these movements to occur. The presence of well-resolved β -relaxation peak with high activation energy of 76.3 kJ/mol for the 50 kGy irradiated sample is interpreted in terms of degradation events that caused cracking of chain segments having high degree of polymerization.

The authors gratefully acknowledge and thank the Department of Physics, Qatar University for allowing them to use their γ -irradiation facility. MKH would like to acknowledge the Qatar

University's financial support through the Center for Advanced Materials' Start-Up grant.

The authors have declared no conflicts of interest.

5 References

- Reier, G. E., Shangraw, R. F., Microcrystalline cellulose in tableting. *J. Pharm. Sci.* 1966, *55*, 510–514.
- Webery, C. J., Haugaard, V., Festersen, R., Bertelsen, G., Production and applications of biobased packaging materials for the food industry. *Food Addit. Contam.* 2002, *19*, 172–177.
- Wüstenberg, T., *Cellulose and Cellulose Derivatives in the Food Industry: Fundamentals and Applications*, Wiley-VCH, Weinheim, Germany 2014.
- Bajwa, S. G., Bajwa, D. S., Holt, G., Optimal substitution of cotton burr and linters in thermoplastic composites. *Forest Prod. J.* 2009, *59*, 40–46.
- Pathan, N. K., Al-Maadeed, M. A., Improvement of ternary recycled polymer blend reinforced with date palm fibre. *Mater. Des.* 2014, *60*, 532–539.
- Crawford, R. L., *Lignin Biodegradation and Transformation*, John Wiley and Sons, New York 1981.
- Klemm, D., Heublein B., Fink, H. P., Bohn, A., Cellulose: Fascinating Biopolymer and sustainable raw material. *Angew. Chem., Int. Ed.* 2005, *44*, 3358–3393.
- Fengel, D., Wegener, G., *Wood: Chemistry, Ultrastructure, Reactions*, De Gruyter, Berlin, Germany 1989.
- Biganska, O., Navard, P., Kinetics of precipitation of cellulose from cellulose–nmmo–water solutions. *Biomacromolecules* 2005, *6*, 1948–1953.
- Ass, B. A. P., Belgacem, M. N., Frollini, E., Mercerized linters cellulose: Characterization and acetylation in N,n-dimethylacetamide/lithium chloride. *Carbohydr. Polym.* 2006, *63*, 19–29.
- Liu, Z., Wang, H., Li, Z., Lu, X., et al., Characterization of the regenerated cellulose films in ionic liquids and rheological properties of the solutions. *Mater. Chem. Phys.* 2011, *128*, 220–227.
- Zhang, L., Ruan, D., Zhou, J., Structure and properties of regenerated cellulose films prepared from cotton linters in NaOH/urea aqueous solution. *Ind. Eng. Chem. Res.* 2001, *40*, 5923–5928.
- Li, R., Zhang, L., Xu, M., Novel regenerated cellulose films prepared by coagulating with water: Structure and properties. *Carbohydr. Polym.* 2012, *87*, 95–100.
- Chmielewski, A. G., Saeid, M. H., Ahmed, S., Progress in radiation processing of polymers. *Nucl. Instrum. Methods Phys. Res. B* 2005, *236*, 44–49.
- Al-Maadeed, M. A., Change in structure of ultrahigh molecular weight polyethylene due to irradiation in air and in nitrogen. *Int. J. Polym. Anal. Charact.* 2006, *11*, 71–84.
- Rajvaidya, S., Bajpai, R., Bajpai, A. K., Effect of gamma irradiation on the interpenetrating networks of gelatin and polyacrylonitrile: Aspect of Crosslinking using microhardness and crosslink density measurements. *J. Appl. Polym. Sci.* 2006, *101*, 2581–2586.
- Lamanna, M., Morales, N. J., Garcia, N. L., Goyanes, S., Development and characterization of starch nanoparticles by

- gamma radiation: Potential application as starch matrix filler. *Carbohydr. Polym.* 2013, 97, 90–97.
- [18] Khan, R. A., Salmieri, S., Sharmin, N., Dussault, D., et al., Fabrication and mechanical characterization of biodegradable and synthetic polymeric films: Effect of gamma radiation. *Radiat. Phys. Chem.* 2012, 81, 995–998.
- [19] Vanichvattanadecha, C., Supaphol, P., Nagasawa, N., Tamada, M., et al. Effect of gamma radiation on dilute aqueous solutions and thin films of N-succinyl chitosan. *Polym. Degrad. Stabil.* 2010, 95, 234–244.
- [20] Zhang, X., Xu, L., Huang, X., Wei, S., et al., Structural study and preliminary biological evaluation on the collagen hydrogel crosslinked by Γ -irradiation. *J. Biomed. Mater. Res.* 2012, 100, 2960–2969.
- [21] Takacs, E., Wojnarovits, L., Foldvary, C., Hargittai, P., et al., Effect of combined gamma-irradiation and alkali treatment on cotton-cellulose. *Radiat. Phys. Chem.* 2000, 57, 399–403.
- [22] Vázquez, M. I., Galan, P., Casado, J., Ariza, M. J., et al., Effect of radiation and thermal treatment on structural and transport parameters for cellulose regenerated membranes. *Appl. Surf. Sci.* 2004, 238, 415–422.
- [23] Hassan, M. K., Wiggins, J. S., Storey, R. F., Mauritz, K. A., Broadband dielectric spectroscopic characterization of the hydrolytic degradation of carboxylic acid-terminated poly(D, L-lactide) materials. *Polymer* 2007, 48, 2022–2029.
- [24] Rhoades, D. W., Hassan, M. K., Osborn, S. J., Moore, R. B., et al., Broadband dielectric spectroscopic characterization of Nafion[®] chemical degradation. *J. Power Sources* 2007, 172, 72–77.
- [25] Osborn, S. J., Hassan, M. K., Divoux, G. M., Rhoades, D. W., et al., Glass transition temperature of perfluorosulfonic acid ionomers. *Macromolecules* 2007, 40, 3886–3890.
- [26] Kremer, F., Schönhals, A., *Broadband Dielectric Spectroscopy*, Springer, Berlin, Germany 2003, p. 225.
- [27] Mauritz, K. A., Stefanithis, I. D., Microstructural evolution of a silicon oxide phase in a perfluorosulfonic acid ionomer by an in situ sol-gel reaction. 2. Dielectric relaxation studies. *Macromolecules* 1990, 23, 1380–1388.
- [28] Havriliak, S., Negami, S., A complex plane analysis of α -dispersions in some polymer systems. *J. Polym. Sci., Part C: Polym. Symp.* 1966, 14, 99–117.
- [29] Havriliak, S., Negami, S., A complex plane representation of dielectric and mechanical relaxation processes in some polymers. *Polymer* 1967, 8, 161–210.
- [30] Negami, S., Ruch, R. J., Myers, R. R., The dielectric behavior of poly(vinyl acetate) as a function of molecular weight. *J. Colloid Interface Sci.* 1982, 90, 117–126.
- [31] Kremer, F., Schönhals, A., *Broadband Dielectric Spectroscopy*, Springer, Berlin, Germany 2003, pp. 64.
- [32] Kamide, K., Okajima, K., Kowsaka, K., Dissolution of natural cellulose into aqueous alkali solution: Role of super-molecular structure of cellulose. *Polym. J.* 1992, 24, 71–86.
- [33] Iler, E., Kukielka, A., Stupinska, H., Mikolajczyk, W., Electron-beam stimulation of the reactivity of cellulose pulps for production of derivatives. *Radiat. Phys. Chem.* 2002, 63, 253–257.
- [34] Charlesby, A., *Atomic Radiation and Polymers*, Pergamon Press, Oxford, UK 1960.
- [35] Pruzinec, J., Kadlecik, J., Varga, S., Pivovarnicek, F., Study of the effect of high-energy radiation on cellulose. *Radiochem. Radioanal. Lett.* 1981, 49, 395–403.
- [36] Khan, R. A., Beck, S., Dussault, D., Salmieri, S., et al., Mechanical and barrier properties of nanocrystalline cellulose reinforced poly(caprolactone) composites: Effect of gamma radiation. *J. Appl. Polym. Sci.* 2013, 129, 3038–3046.
- [37] Ibrahim, S. M., Characterization, mechanical, and thermal properties of gamma irradiated starch films reinforced with mineral clay. *J. Appl. Polym. Sci.* 2011, 119, 685–692.
- [38] Einfeldt, J., Kwasniewski, A., Characterization of different types of cellulose by dielectric spectroscopy. *Cellulose* 2002, 9, 225–238.
- [39] Saad, G. R., Sakamoto, M., Furuhashi, K., Dielectric study of β -relaxation in some cellulosic substances. *Polym. Int.* 1996, 41, 293–299.
- [40] Montes, H., Cavaillé, J. Y., Mazeau, K., Secondary relaxations in amorphous cellulose. *J. Non-Cryst. Solids* 1994, 172, 990–995.